J Mater Sci (2009) 44:778–785
DOI 10.1007/s10853-008-3141-9

Evaluation of elastic properties of reduced NiO-8YSZ anode-supported bi-layer SOFC structures at elevated temperatures in ambient air and reducing environments

S. Biswas · T. Nithyanantham · N. T. Saraswathi · S. Bandopadhyay

Received: 4 August 2008 / Accepted: 26 November 2008 / Published online: 27 December 2008

Abstract Elastic properties of Ni-8YSZ anode-supported bi-layer SOFC structures were studied at elevated temperatures up to 1,000 °C in both ambient air and H_2 environments. The anode samples with desired porosity and microstructure were fabricated by reducing a NiO-8YSZ anode precursor structure in a gas mixture of 5% H_2–95% Ar at 800 °C for selected time periods up to 8 h. The development of the essential porous microstructure in forming the Ni-8YSZ cermet phase was analyzed with SEM. It was observed that the room temperature elastic moduli and hardness of the anode samples decrease significantly with increasing fraction of reduced NiO. Since the elastic properties of fully dense Ni, NiO, and 8YSZ are comparable to each other, the decrease in the magnitude in elastic moduli and hardness is evidently due to the colossal increase in porosity in the reduced Ni-8YSZ cermet anodes because of the reduction of NiO to Ni. At elevated temperatures, the Ni-8YSZ anodes show a complex profile of Young's modulus as a function of temperature, which is significantly different from the unreduced NiO-8YSZ samples. When studied in ambient air, the Young's modulus of the Ni-8YSZ samples decrease slowly up to ~250 °C, then more rapidly from 250 to 550 °C, and finally it increases monotonically with the increase in temperature. However, in reducing environment, the Young's moduli values decrease continuously throughout the temperature range. Two sets of samples of different thicknesses were studied simultaneously to highlight the effects of the sample thickness on the elastic properties of the anodes.

S. Biswas · T. Nithyanantham · N. T. Saraswathi · S. Bandopadhyay (✉)
College of Engineering and Mines, University of Alaska, Fairbanks, AK 99775, USA
e-mail: ffs0b@uaf.edu

Introduction

Mechanical stability over long-term operation at elevated temperatures in reactive fuel environments is one of the most stipulating aspects for the development of solid oxide fuel cells (SOFCs) as a highly reliable and affordable source of clean energy [1–8]. Successful commercialization of SOFCs depends not only on the electrochemical efficiency of its components but also on its ability to endure the mechanical stresses that arises during fabrication, stack assembling, or the extensive servicing period when it is susceptible to external impacts and internal thermo-mechanical stresses. To withstand the mechanical affects and for the structural integrity of the SOFC stack, at least one of the SOFC components should have adequate thickness and mechanical robustness to provide the structural support to the cell. Although the conventional electrolyte-supported SOFC designs offer desired mechanical strength, the thick electrolyte layer deleteriously affects the performance of the cell by increasing the ohmic losses, operating temperature, start-up time and overall cost [3, 6].

In an attempt to overcome the challenges with electrolyte-supported SOFCs, Ni-Y_2O_3 stabilized ZrO_2 (Ni-YSZ) porous cermet-based anode-supported cells have been successfully developed in both tubular and planar type designs. Ni-YSZ is favored due to its enviable properties of excellent electro-catalytic activity for the H_2 oxidation reaction at the triple phase boundary (TPB) among Ni, YSZ, and gaseous H_2 [9, 10], high electronic and ionic

conductivity [11], high mechanical stability and compatibility with YSZ electrolyte [12], and structural stability at high operating temperatures in H_2 atmosphere [11, 13]. The structural integrity of the anode is maintained by the porous YSZ framework that allows H_2 to diffuse through the cermet, thereby extending the TPB into part of the electrode volume, rather than limiting it to the contact interface with the electrolyte. Moreover, YSZ keeps the Ni particles dispersed by preventing them from agglomeration due to sintering during service. Enhanced electro-catalytic activities in the highly porous Ni-based anode generate high external current densities while keeping internal current densities and over potentials low. Therefore, it is highly desirable that the anode layer should have sufficient porosity and high electronic–ionic conductivity without sacrificing the mechanical strength. Mechanical strength of the anode will increase with the increase in the YSZ content. However, high YSZ concentration would eventually results in low electrical conductivity, which depends on the extent of percolation of the metallic Ni phase. The mechanical stability and electro-catalytic activities of Ni-YSZ anode structure is crucially dependent on the phase distribution and microstructure in the cermets. For optimum performance of the anode, at least 40 vol.% of Ni [14, 15] is required along with a homogeneous distribution of Ni and YSZ phases [16]. It has been observed that smaller particle size, either Ni or YSZ, is advantageous in obtaining superior mechanical strength and electrochemical performance [6, 7]. However, enlarging the YSZ particle size helps to diminish the stresses resulting due to mismatches in the coefficient of thermal expansion (CTE) at the anode–electrolyte interface [6, 16].

Study of mechanical properties of SOFC components is essential to comprehend the reliability issues, which depend on several factors, i.e., residual stresses, chemical stresses arising due to reduction–oxidation reactions, assembly stresses, stresses generated by thermal cycling, etc. Usually, the Ni-YSZ anode layer is fabricated from a NiO-YSZ anode precursor structure, which is tape cast from powder slurries and co-sintered with the electrolyte layer. Residual stresses in such laminates results primarily from the CTE mismatch between the anode and electrolyte layers. During first service cycle of operation or conditioning, when hydrogen fuel is introduced to the cell, NiO-YSZ is reduced into a Ni-YSZ cermet. This reduction reaction results in a drastic change in porosity and density of the anode layer as well as its physical and mechanical properties. The process introduces mismatch stresses in the SOFC stack, which in turn have an appalling effect on the structural integrity of the SOFC [1, 2, 4–6]. Internal stresses may also build-up due to thermal shocks generated by the thermal cycling effects during start-up/shut-down operations of the SOFC. Several studies have been reported on porosity and temperature dependent mechanical properties of Ni-YSZ anode-supported SOFCs. Flexural strength of YSZ electrolyte and Ni-YSZ anode is evaluated at ambient and elevated temperatures with concentric ring-on-ring loading configuration [4, 5, 17–19]; porosity dependent elastic properties have been reported [1, 2, 4, 5]; fracture toughness is measured by both indentation fracture and double torsion loading methods [4, 5, 17–19]. However, there are few reports on the evaluation of elastic properties of Ni-YSZ anodes at elevated temperatures and reducing environments, simulating the actual operating conditions in SOFCs. To optimize the anode design, it is also necessary to study the effects of anode layer thickness on the overall mechanical stability of the SOFC membrane electrolyte assembly.

In this paper, we report a systematic study of the elastic properties, i.e., Young's modulus (E) and shear modulus (G) of reduced NiO-8YSZ anode-supported bi-layer structures of planar type SOFCs at ambient and elevated temperatures in both air and hydrogen environments. The results are analyzed in correlation with cermet phase formation and development of the desired microstructure. Two sets of specimens of different thicknesses were studied concurrently to investigate the dependence of the hardness and the elastic properties on the thickness of the Ni-8YSZ cermet anodes.

Experimental

The two batches of square shaped samples (4 in. × 4 in.) of 600 and 900 μm thicknesses were supplied by Materials and Systems Research, Inc., USA. In both batches, the square laminates have a dense electrolyte layer (~8 μm thickness) of 8YSZ supported by the thick NiO-8YSZ (70:30 vol.%) anode precursor layer. The anode–electrolyte bi-layer structures were formed by depositing the thin 8YSZ electrolyte layer over the NiO-8YSZ anode layer formed by tape casting of powder slurries and then co-sintered at ~1,100 °C. The as-received samples were cut into suitable sizes and reduced in a gas mixture of 5% H_2–95% Ar at 800 °C. The reduction was carried out in an autoclave set-up, where the samples were treated at that temperature for 1 h prior to the initiation of the reduction reaction. The gas mixture was introduced in the chamber at a constant flow rate of 3.2 SLPM and the temperature–chemical environment condition was maintained for selected time periods up to 8 h. Finally, the samples were cooled down to room temperature without changing the reducing gaseous environment.

The porosity and density of as-received and the reduced anode-supported bi-layer samples were estimated by Archimedes principle as described in ASTM Standard

C20-00. Since the thickness of the electrolyte layer is negligible in comparison to the anode, the derived values are near approximation of the true values of porosity/density in the anode. As described in an earlier report [20], the fraction of NiO reduced in the samples was determined by thermo gravimetric analysis (TGA) carried out in air with an analyzer of Perkin-Elmer model DT-40, Shimadzu Co., Japan. The microstructures were studied by a JEOL JSM-7000 scanning electron microscope (SEM) with in situ energy dispersive spectroscopy (EDS) facilities. An accelerating voltage of 10 kV was used to resolve the images of the Ni-YSZ cermet structure. Hardness of the samples was measured by Vicker's indentation method on the anode surface with an applied load of 500 g for 15 s. Young's and shear moduli of the as-received, partially and fully reduced samples were determined by the impulse excitation technique using the Buzz-o-sonic software (BuzzMac, Glendale, WI) by measuring the fundamental vibration frequencies using a custom made experimental set-up.

Results and discussion

Structural changes during reduction

The fraction of reduced NiO, r (%), and the porosity, P (%), measured in the reduced samples are plotted in Fig. 1a, as a function of reduction time. The reduction kinetics is similar in both sets of samples (curves a and b). In the first stage, the reduction speed is very fast, and the curves are very steep. This evidently suggests that the first few hours in reducing the NiO in the anode are the most crucial period as 2 h of exposure to the reducing conditions is enough to reduce ~80% of NiO in the samples. In the second stage, the reduction speed decreases gradually, and further exposure to the reducing conditions could only cause very marginal increase in r. After 8 h of exposure, the value of r becomes 81.3% (600 μm thick samples) or 82.2% (900 μm thick samples). As expected, the reduction mechanism in the anode layers has drastically changed the porosity in the samples (curves c and d). In the 600 μm thick samples, the porosity has increased from a value of 12% (density, $\rho = 5.47$ g/cc) in the as-received samples to 36.68% ($\rho = 4.69$ g/cc) in the 8 h reduced samples while the values are 11.76% ($\rho = 5.24$ g/cc) and 39.66% ($\rho = 4.50$ g/cc) in the as-received and 8 h reduced 900 μm thick samples, respectively. Assuming the dimensional change in the anode support layer due to the reduction to be negligible, the relative bulk density of the fully reduced Ni-8YSZ samples would be ~85% of that of as-received NiO-8YSZ samples containing 70 vol.% NiO due to the difference in the molar volume of NiO (11.2 cm^3 mol^{-1})

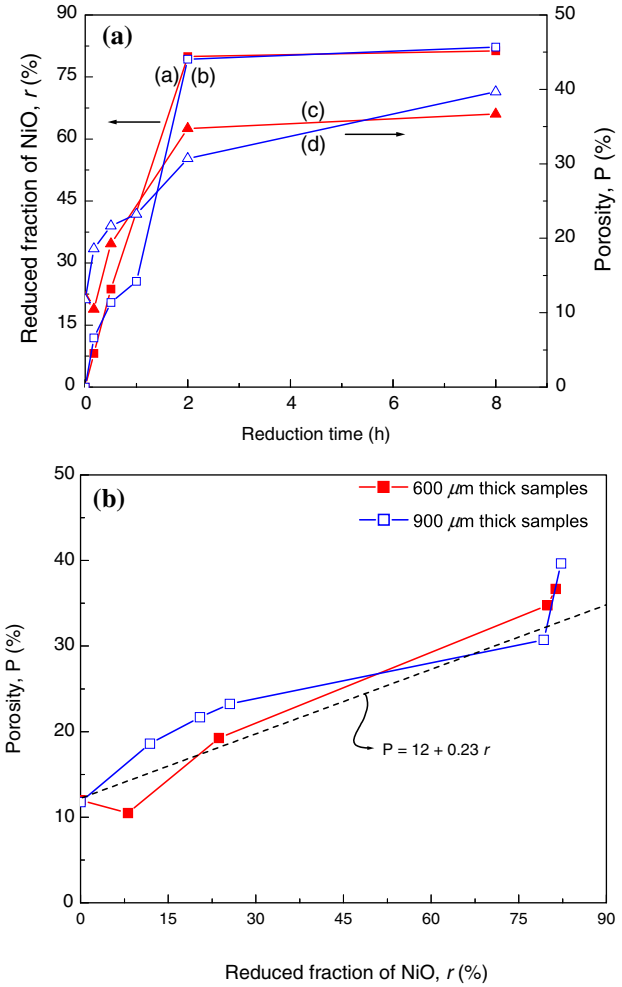

Fig. 1 **a** Reduced fraction of NiO, r (a and b), and the measured value of porosity, P (c and d), as a function of reduction time in the reduced NiO-8YSZ anode samples of 600 and 900 μm thicknesses, respectively, and **b** the derived relationships between P and r in the two sets of samples

and Ni (6.6 cm^3 mol^{-1}) [7]. The derived values of bulk densities in the two sets of as-received and reduced samples are consistent with the calculated values. This indicates that the YSZ framework has little effect on the reduction process at that temperature and the increase in porosity is assumed to be only from the volumetric change by the reduction of NiO to Ni. As reported by Radovic and Lara-Curzio [4, 5], the porosity, P (%), in the anode can be expressed as a function of r, in the following manner:

$$P = P_0 + \rho_0 m_{\mathrm{NiO}}[(1/\rho_{\mathrm{NiO}}) - (1/\rho_{\mathrm{Ni}}) + (M_{\mathrm{O}}/M_{\mathrm{NiO}})(1/\rho_{\mathrm{Ni}})]r, \quad (1)$$

where P_0, ρ_0, m_{NiO}, ρ_{NiO}, ρ_{Ni}, M_{O}, and M_{NiO} are the initial porosity, initial density, initial weight fraction of NiO, density of pure NiO, density of pure Ni, atomic weight of oxygen (16 amu), and molecular weight of NiO (74.7 amu),

respectively. Neglecting the minor differences in the values of P_0 and ρ_0 in the two sets of samples and inserting the constants, $\rho_{Ni} = 8.88$ g/cc, $\rho_{NiO} = 6.67$ g/cc, and $m_{NiO} = 0.7128$ (converting 70 vol.% into wt%), the following relationship is obtained:

$$P = 12 + 0.239r. \quad (2)$$

A comparison between Eq. 2 and the derived relationships between P and r in the two sets of samples (Fig. 1b) suggests reasonable agreement of this model with experimentally obtained values.

The increase in porosity from the reduction severely affects the hardness of the anode support layer. As shown in Fig. 2, a Vickers's hardness value of 5.5 GPa in the as-received 600 μm thick samples ($P = 12\%$) is reduced to less than 1 GPa in the 8-h reduced samples with an increased value of $P = 36.68\%$. Similarly, in 900 μm thick samples, the hardness value of 3.13 GPa in the as-received anode layer reduces to ~0.40 GPa in the 8-h reduced Ni-8YSZ samples. It is also observed that the scattering in the hardness values decreases with increasing porosity. Even though they are highly porous, the 2- or 8-h reduced anode samples have negligible scattering in their hardness values in comparison to the as-received samples. This type of behavior is attributed to the enhanced plasticity due to higher Ni metal content present in the highly reduced porous anodes [13]. Another interesting observation is the decrease in the overall hardness of the anode support layer with the increase in its thickness. Although a thicker anode layer enhances the electro-catalytic activities, the decrease in the hardness would eventually reduce the mechanical stability of the SOFC stack.

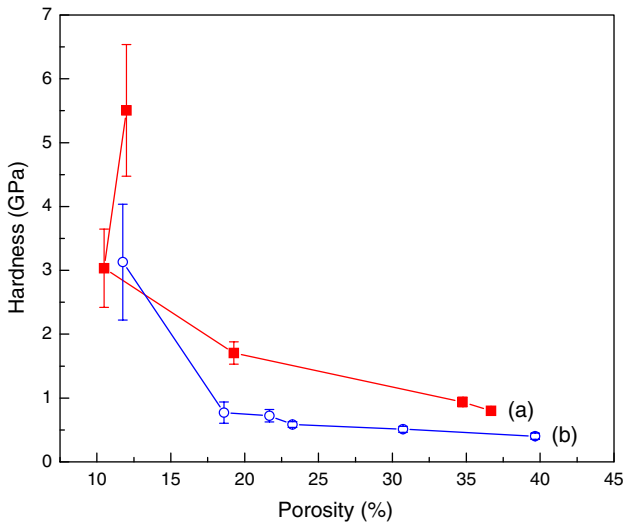

Fig. 2 Hardness values plotted as a function of porosity in the as-received and the reduced (a) 600 μm and (b) 900 μm thick samples, respectively

In Fig. 3, the typical SEM micrographs illustrate a systematic study of the effect of reduction on the development of microstructure in forming the Ni-8YSZ cermet anodes. In both sets of samples, the as-received NiO-8YSZ anode precursor (Fig. 3a and a′) is fairly dense with few pores, which are neither uniformly distributed nor having regular shapes. Most of the pores have a dimension of 0.8–1.2 μm. In addition, few bigger void regions (2–6 μm) is also observed in both sets of samples, which have been formed possibly due to the agglomeration of the particles of carbon pore former during synthesis and created after sintering. During the initial stage of the exposure to the reducing conditions, the reduction reaction starts at the surface of the NiO particles. As a result, a thin surface layer of Ni is formed on the NiO particles, which gradually grows until the whole NiO particle is reduced to Ni. Figure 3b and b′ show the microstructure of the partially reduced anode samples after 30 min of exposure. A shining surface layer of Ni can be observed at the edges of the NiO particles. Further exposure to the reducing conditions has reduced the total volume of NiO significantly, as exhibited by the changes in the microstructure in the 8-h reduced samples (Fig. 3c and c′), which leads to the development of a typical porous cermet microstructure of homogeneous distribution of Ni particles in 8YSZ with interconnected pore network. It is observed that the pores that were formed due to shrinkage of NiO particles during their reduction into Ni (1.2–2 μm) are much bigger than those initially present in NiO-8YSZ samples (0.8–1.2 μm). However, the bigger void regions remain almost unaffected. There is no significant difference in the microstructure of the two sets of fully reduced Ni-8YSZ anode samples.

Several investigations of the process of hydrogen oxidation reaction in Ni-8YSZ cermet anodes revealed that the reaction is indeed limited in the TPB region [9, 10, 21]. The possible electrochemical processes in the hydrogen → water reaction at the TPB regions are solid-state diffusion, surface diffusion, and adsorption in the electrode/electrolyte surfaces and interface. High electrical power is obtained through high conversion rates (electrochemical reaction rates) leading to high current densities at low overpotentials. High conversion rate requires highly active anodes (high electro-catalytic activity) with high amount of TPB contacts. The formation of the desired porous microstructure of Ni-8YSZ is very crucial for the development of efficient anodes [6, 11]. The homogeneous distribution of electron conducting Ni with oxygen ion conductor 8YSZ disperses the reaction zones in the volume of the porous electrode. Spreading out the reaction zones away from the anode/electrolyte interface enhances the electrochemical conversion rates. The uniformly distributed interconnected pores in the Ni-8YSZ anode provide unbroken percolation paths for electrons, oxide ions, and

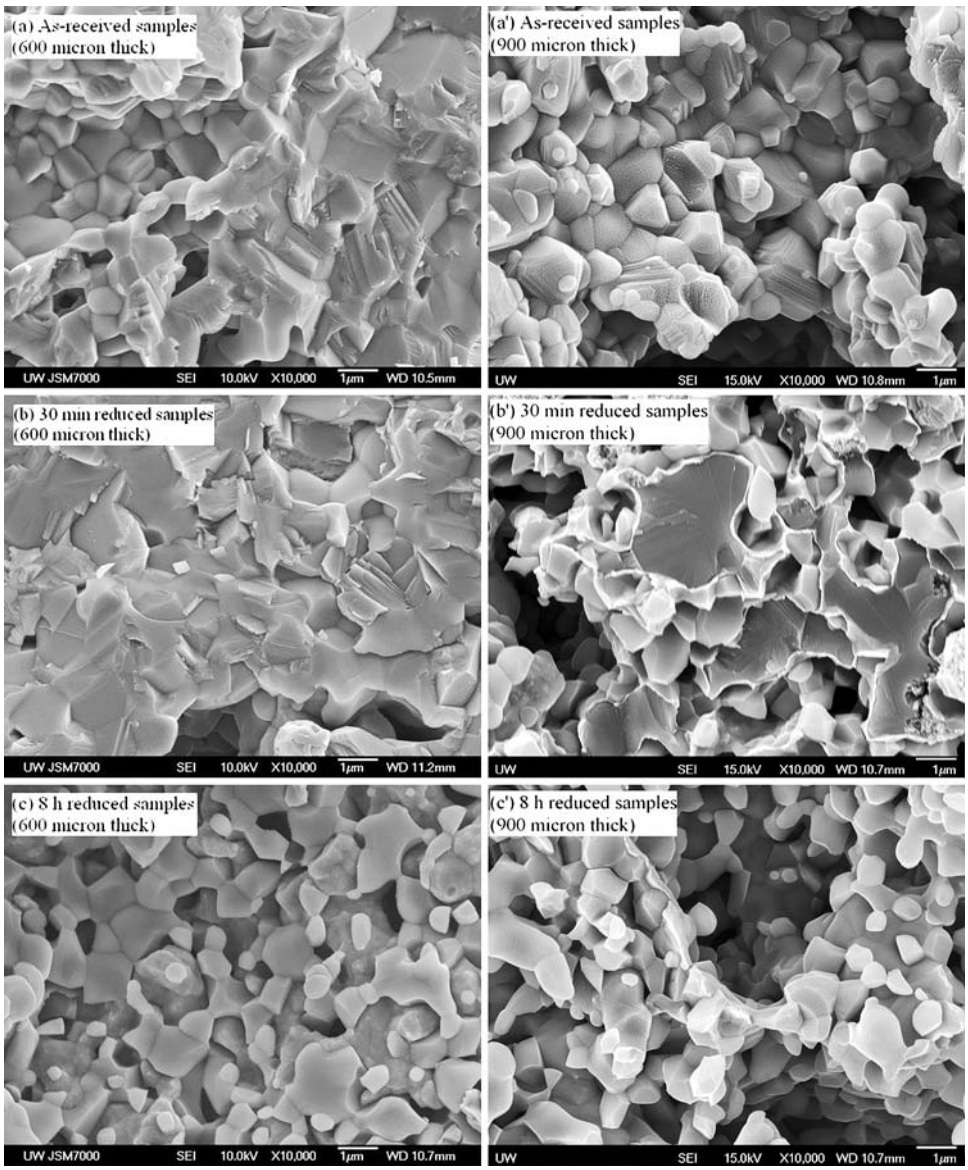

Fig. 3 SEM micrographs in the anode surface of (a and a′) as-received, (b and b′) 30 min, and (c and c′) 8-h reduced NiO-8YSZ samples of 600 and 900 μm thicknesses, respectively

hydrogen fuel. On the other hand, the required mechanical strength and structural integrity of the anode is maintained by the 8YSZ framework. The high-temperature sintering (∼1,100 °C) of the green anode precursor structure after its deposition results the essential densification and neck formation between the particles in the anode, highly necessary for the formation of percolation paths. Therefore, the performance and mechanical stability of the Ni-8YSZ anode vastly depends on the sintering of a well-packed green structure to obtain a mechanically rigid YSZ network capable of restricting the Ni phase from agglomeration during operation. The Ni phase controls the thermal expansion of the Ni-8YSZ cermet with its high thermal conductivity and plasticity, and results to a high thermal shock resistance [13].

Elastic properties of reduced NiO-8YSZ anodes

The elastic properties of NiO-8YSZ anodes are dependent on several factors, i.e., microstructure (porosity and particle size), composition, temperature, physical dimension, etc. [1–5]. The changes in the elastic properties in the anodes from the reduction during the first service cycle of operation have considerable effects on the distribution of residual stresses in the SOFC components. In addition, the thermal cycling effects during start-up/shut-down operations highly influence the elastic behavior thereby leading to a re-distribution in the stresses. Therefore, a detailed analysis of the elastic properties of the anode is necessary to predict the conditions for optimal performance and reliability of the SOFC. Although, there are

few reports on the effect of porosity on the elastic properties of anodes, there is hardly any report on the temperature dependent elastic properties of Ni-based SOFC anodes in actual operating conditions. At elevated temperatures, in addition to the effects of porosity, the onset of oxidation or other physical processes in the Ni-8YSZ cermets influences the elastic behavior significantly.

In Fig. 4, the Young's (E) and shear (G) moduli of as-received and the reduced NiO-8YSZ anodes, characterized with the impulse excitation technique at room temperature, are plotted as a function of volume fraction of porosity in the samples. The measured values of Young's and shear moduli in the as-received samples are found to be 119.2 and 48.8 GPa (600 μm thick samples), and 107.1 and 74.2 GPa (900 μm thick samples), respectively. The elastic moduli values diminish significantly with the increase in the volume fraction of porosity and becomes $E = 73.4$ and $G = 32.8$ GPa (600 μm thick samples), and $E = 51.2$ and $G = 34.2$ GPa (900 μm thick samples), respectively, in the two batches of 8-h reduced samples. The observed decrease in elastic moduli is evidently due to the changes in the composition of the anode and/or increase in porosity [4–6]. Since, the elastic moduli of fully dense Ni ($E = 200$ GPa and $G = 77$ GPa) [22], NiO ($E = 220$ GPa and $G = 84$ GPa) [22], and 8YSZ ($E = 220$ GPa and $G = 83.3$ GPa) [1, 2] are comparable to each other, the changes in the chemical composition of the anode after reduction is expected to have trivial effects on the magnitude of the effective elastic moduli of the reduced anode material. Therefore, the observed decrease in the elastic moduli in the Ni-8YSZ anode samples is predominantly due to the significant increase in porosity in the samples. It is also observed that a 50% increase in thickness in the samples, has significantly diminished the Young's modulus of the samples. However, the shear moduli values remain approximately the same in the highly reduced samples irrespective of their thickness.

The dependence of elastic moduli on porosity has been characterized by several authors by employing both theoretical (composite sphere method) and empirical (exponential, nonlinear, and linear) models. Selcuk and Atkinson [1, 2] reported similar type of porosity dependence of elastic moduli at room temperature in 75 mol.% NiO-YSZ anode samples containing as much as 14% porosity. Analogous results were also obtained by Radovic and Lara-Curzio [4, 5] in 75 mol.% NiO-YSZ samples with 23% initial porosity. Based on their empirical model, they predicted that the difference in the elastic moduli between hypothetical fully dense NiO-YSZ and Ni-YSZ is $\leq$4%. Therefore, the observed colossal decrease in elastic moduli [$\Delta E \sim 38\%$, $\Delta G \sim 33\%$ (600 μm thick samples) and $\Delta E \sim 52\%$, $\Delta G \sim 54\%$ (900 μm thick samples)] after 8 h of reduction of the two sets of samples is primarily due to the significant increase in porosity with the reduction of NiO.

In addition to porosity, the high operating temperature significantly influences the elastic moduli of the Ni-8YSZ cermet anodes. Figure 5 shows the Young's moduli of as-received and the 8-h reduced anodes of both batches as a function of temperature in ambient air up to 1,000 °C. The temperature dependence of E can be discussed based on the composition of the anodes. The as-received NiO-8YSZ samples, which have NiO as one of the major constituents (70 vol.%) show a distinctively different elastic behavior profile throughout the temperature range (curves a and b),

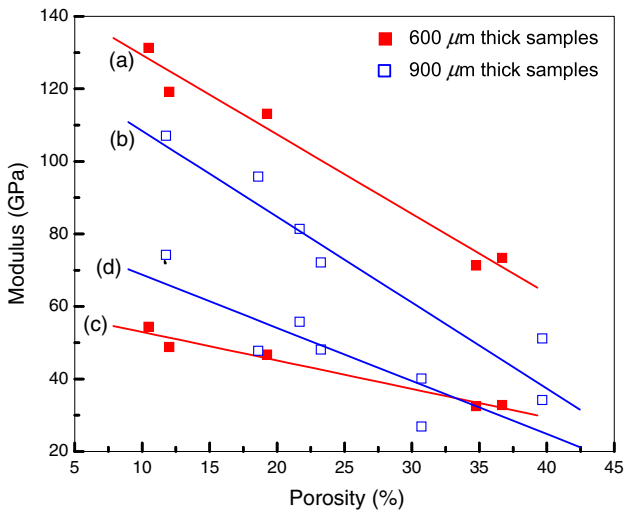

Fig. 4 Room temperature Young's (a, b) and shear (c, d) moduli values plotted as a function of porosity in the samples of 600 and 900 μm thicknesses, respectively

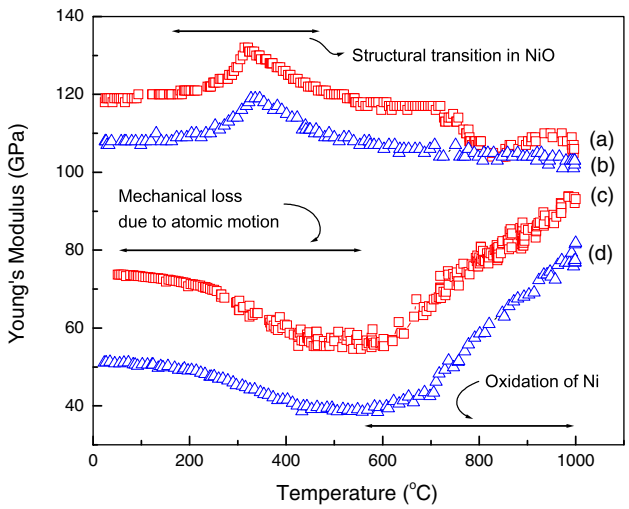

Fig. 5 The variation of Young's modulus with temperature (measured in ambient air) in (a, b) as-received and (c, d) 8-h reduced NiO-8YSZ samples of 600 and 900 μm thicknesses, respectively

from the reduced Ni-8YSZ cermets that have negligible amount of NiO (curves c and d). The high NiO containing as-received samples (both batches) show the steady value of room temperature Young's modulus up to 150 °C. As the temperature increases, an increase in E is observed over 200–500 °C with a maximum value at ~325 °C, prior to a broad decline with further increase in temperature. The increment in E value over this temperature region is related to the structural transition of NiO from distorted face-centered rhombohedral to cubic rock salt structure near its Neel temperature of 250 °C [23, 24]. This structural transition affects many material properties of NiO, including the CTE. An increase in the thermal expansion behavior at ~250 °C is observed in the as-received NiO-8YSZ samples. Above 500 °C, the decrease in Young's moduli values of the NiO rich as-received samples becomes slow and shows a broad decline up to 1,000 °C.

No such structural transition assisted change in the modulus curve can be observed in the 8-h reduced Ni-8YSZ anodes having very negligible amount of NiO in their composition. The observed behavior is rather different and can be divided in to three separate regions. From room temperature to ~250 °C, E decreases slowly, and then more strongly from 250 to 550 °C; finally, it increases monotonically with the increase in temperature. Similar type of temperature dependence of elastic moduli has been observed in ZrO_2 samples stabilized with various dopants [25–28]. The decrease in E values with temperature up to 550 °C is presumably from the mechanical losses due to enhanced atomic motion [29, 30]. The mechanical losses are often responsible for large scattering in E values at higher temperatures. As studied by Weller et al. [31, 32], the internal friction of stabilized cubic zirconia as a function of temperature shows a characteristic doublet structure at ~130 °C corresponding to a singlet structure in tetragonal zirconia with 3 mol.% Y_2O_3. They assigned the doublet peaks to the reorientation jumps of the pairs $V_o^{\bullet\bullet}$–Y_{zr}' representing the elastic and electric dipoles and to the relaxation of oxygen vacancies within a cluster of two or more yttrium ions. This loss of energy is dominant in the temperature range from 150 to 550 °C resulting in a large decrease in the E values of 8YSZ together with a scattering in the values (more prominent in the 600 μm thick samples). However, few authors mentioned the role of elastic anisotropy responsible for the decrease in elastic moduli with temperature [33, 34].

These effects were also present in the as-received NiO-8YSZ samples, but the overlapping of the affects due to the structural transition of NiO makes them dormant. Above 500 °C, the slow decline in E values of the NiO rich samples is evidently due to the same reason as explained above. However, the reason for the observed sharp decrease after ~725 °C in the 600 μm thick samples is not yet clear. In contrast, the Ni-rich reduced cermets show a monotonically increasing tendency in the elastic moduli values above 550 °C. This is reasonably due to the oxidation of Ni in ambient air atmosphere. The formation of NiO scales over the Ni grains increases the elastic modulus of the anode samples. TGA studies of pure Ni reveals that the oxidation starts at ~600 °C in air. However, in actual operations of SOFCs with hydrogen fuels, the Ni-8YSZ cermet anodes do not undergo the oxidation reaction.

To characterize the effects of reducing atmosphere on the elastic properties of the reduced Ni-8YSZ anodes at elevated temperatures, we further analyzed the samples in 5% H_2–95% Ar environment (Fig. 6). The room temperature Young's moduli values of the 8-h reduced Ni-8YSZ samples are found to be ~73 GPa (600 μm thick samples) and ~52 GPa (900 μm thick samples), the same as in ambient air. As the temperature increases, the E values decrease monotonically until the temperature reaches 1,000 °C. The 600 μm thick samples exhibit a sharp decrease in the moduli values along the entire temperature region, whereas in the 900 μm thick samples the avalanche in the moduli values reaches a plateau at 550 °C and remains stable up to 850 °C, thereafter decreases sharply up to 1,000 °C. The total decrease in the Young's modulus in the reduced Ni-8YSZ samples as the temperature increases from room temperature to 1,000°C in reducing atmosphere is ~44% for the 600 μm thick samples and ~40% for the 900 μm thick samples, respectively.

Based on the derived results on the elastic properties of reduced NiO-8YSZ anodes, a detail analysis on the distribution of stresses during SOFC operation is necessary to optimize the SOFC design and predicting its reliability.

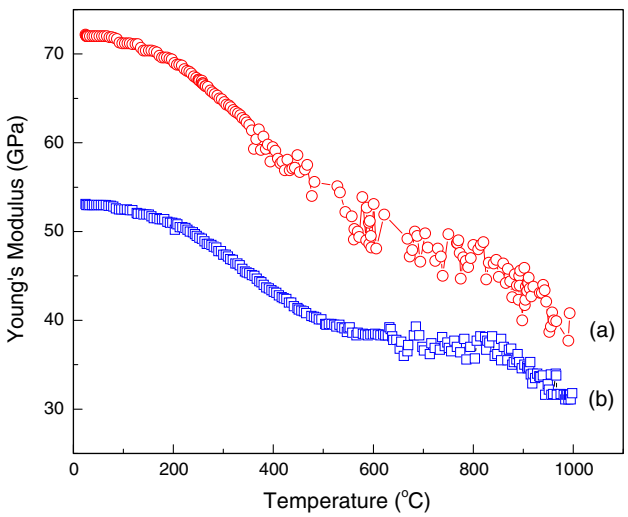

Fig. 6 Young's moduli values of 8-h reduced (a) 600 μm and (b) 900 μm thick NiO-8YSZ samples, as a function of temperature in 5% H_2–95% Ar atmosphere

Conclusions

Highly porous Ni-8YSZ anode/8YSZ electrolyte bi-layer SOFC structures were developed (by reducing a NiO-8YSZ/8YSZ precursor) and studied to characterize the effects of porosity, composition, temperature, and sample thickness on their hardness and elastic properties.

The porosity in the anode samples, which increases with the increase in the fraction of reduced NiO, severely affects the hardness and elastic moduli of the samples. It was found that a room temperature hardness value of 5.5 GPa in an unreduced precursor sample of 600 μm thickness ($P \sim 12\%$) reduces to less than 1 GPa after 8 h of reduction with an increased value of $P \sim 36.68\%$. Similarly, a decrease of $\sim$38% in the Young's modulus and $\sim$33% in shear modulus was observed at room temperature in the same 8-h reduced samples in comparison to the unreduced anode precursor. Since the elastic properties of fully dense Ni, NiO, and 8YSZ are comparable to each other, the change in composition in the anodes due to the reduction is expected to have trivial effects on the elastic moduli. Therefore, the large decrease in the magnitude of elastic moduli is exclusively due to the colossal increase in porosity in the reduced Ni-8YSZ cermet anodes. At elevated temperatures, in addition to porosity several factors influence the elastic properties significantly. In ambient air, the Young's moduli of the Ni-8YSZ samples decrease slowly up to $\sim$250 °C, then more strongly from 250 to 550 °C (essentially due to the mechanical losses due to enhanced atomic motion), and finally, it increases monotonically with the increase in temperature due to the onset of oxidation in the Ni-8YSZ cermets. In contrast, when studied in reducing environment, the Young's moduli values decrease continuously throughout the temperature range up to 1,000 °C. It could be stated that, with microstructure and porosity approximately the same, a 50% increase in the anode layer thickness would reduce the hardness and Young's modulus of the Ni-8YSZ anodes at room/elevated temperatures in both ambient air and reducing environments.

Acknowledgements This work was carried out with the financial support from the United States Department of Energy project grant # DE-FG36-05GO15194. The authors sincerely thank Materials and Systems Research, Inc., Salt Lake City, USA for providing the samples.

References

1. Selcuk A, Atkinson A (1997) J Eur Ceram Soc 17:1523
2. Selcuk A, Atkinson A (1999) Acta Mater 47:867
3. Gutierrez-Mora F, Ralph JM, Routbort JL (2002) Solid State Ionics 149:177
4. Radovic M, Lara-Curzio E (2004) J Am Ceram Soc 87:2242
5. Radovic M, Lara-Curzio E (2004) Acta Mater 52:5747
6. Wang Y, Walter ME, Sabolsky K, Seabaugh MM (2006) Solid State Ionics 177:1517
7. Yu JH, Park GW, Lee S, Woo SK (2007) J Power Sources 163:926
8. Giraud S, Canel J (2008) J Eur Ceram Soc 28:77
9. Setoguchi T, Okamoto K, Eguchi K, Arai H (1992) J Electrochem Soc 139:2875
10. Jiang SP, Badwal SPS (1997) J Electrochem Soc 144:3777
11. Jiang SP, Chan SH (2004) Mater Sci Tech 20:1109
12. Tsoga A, Naomidis A, Nikolopoulos P (1996) Acta Mater 44:3679
13. Ramanathan S, Krishnakumar KP, De PK, Banerjee S (2004) J Mater Sci 39:3339. doi:10.1023/B:JMSC.0000026934.88520.67
14. Marinek M, Zupan K, Macek J (2000) J Power Sources 86:383
15. Lee JH, Moon H, Lee HW, Kim J, Kim JD, Yoon KH (2002) Solid State Ionics 148:15
16. Zhu WZ, Deevi SC (2003) Mater Sci Eng A Struct Mater 362:228
17. Selcuk A, Atkinson A (2000) Solid State Ionics 134:59
18. Selcuk A, Atkinson A (2000) J Am Ceram Soc 83:2029
19. Radovic M, Lara-Curzio E, Armstrong B, Walls C (2003) Ceram Eng Sci Proc 24:329
20. Nithyanantham T, Saraswathi NT, Biswas S, Bandopadhyay S, J Power Sources (Communicated)
21. de Boer B, Gonzalez M, Bouwmeester HJM, Verweij H (2000) Solid State Ionics 127:269
22. Liu C, Lebrun JL, Huntz AM (1993) Mater Sci Eng A 160:113
23. Samuel Smart J, Greenwald S (1951) Phys Rev 82:113
24. Toussaint CJ (1971) J Appl Cryst 4:293
25. Wachtman JB, Jam DG (1959) J Am Ceram Soc 42:254
26. Sakaguchi S, Murayama N, Kodama Y, Wakai F (1991) J Mater Sci Lett 10:282
27. Adams JW, Ruh R, Mazdiyasni KS (1997) J Am Ceram Soc 80:903
28. Roebben G, Basu B, Vleugels J, van der Biest O (2003) J Eur Ceram Soc 23:481
29. Shimada M, Matsushita K, Kuratani S, Okamoto T, Koizumi M, Tsukuma K, Tsukidate T (1984) J Am Ceram Soc 67:C23
30. Lakki A, Herzog R, Weller M, Schubert H, Reetz C, Gorke O, Kilo M, Borchardt G (2000) J Eur Ceram Soc 20:285
31. Weller M, Herzog R, Kilo M, Borchardt G, Weber S, Scherrer S (2004) Solid State Ionics 175:409
32. Weller M, Khelfaoui F, Kilo M, Taylor MA, Argirusis C, Borchardt G (2004) Solid State Ionics 175:329
33. Ingel RP, Lewis D (1988) J Am Ceram Soc 71:265
34. Rice RW (1994) J Mater Sci Lett 13:1261